Nanosized polypyrrole affected by surfactant agitation for emulsion polymerization

Yusuke Hoshina, Erasto Armando Zaragoza-Contreras, Ramin Farnood & Takaomi Kobayashi

Springer

Springer

ORIGINAL PAPER

Nanosized polypyrrole affected by surfactant agitation for emulsion polymerization

**Yusuke Hoshina · Erasto Armando Zaragoza-Contreras ·
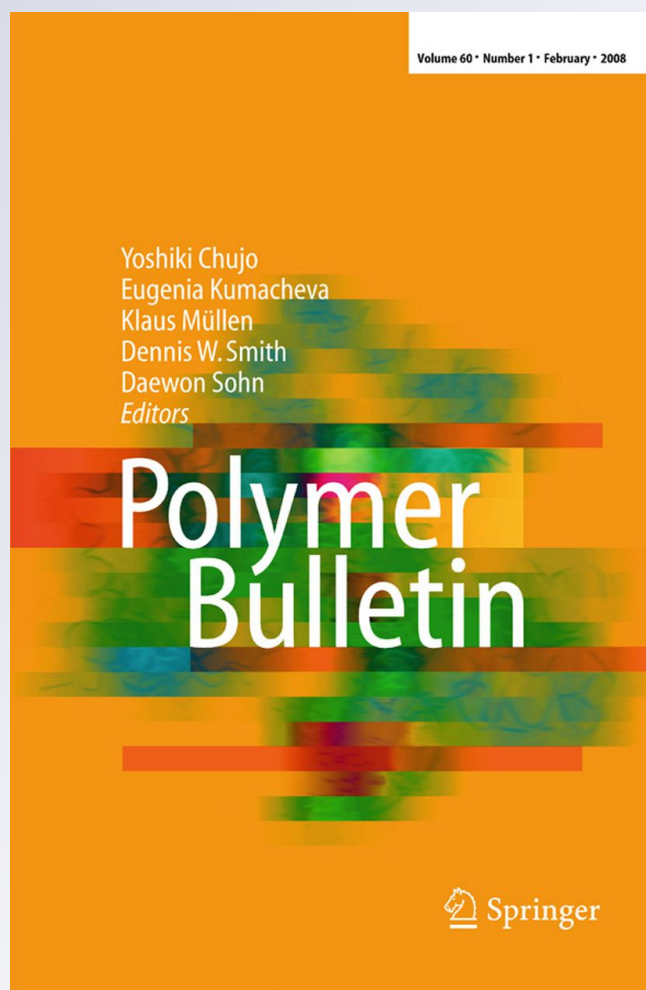Ramin Farnood · Takaomi Kobayashi**

Abstract Nanosized conductive polypyrrole (PPy) powders were prepared using emulsion polymerization with aid of high speed agitation. Different agitation speeds from 650 to 24,000 rpm were used with different anionic, cationic, and non-ionic surfactants. Then, the effects of the agitation speed and surfactant species were examined in terms of their physical and electrical properties of conductivity and powder size. Prepared PPy nanopowders exhibited high conductivity values of 10 S/cm regions, when sodium dodecylbenzenesulfonate (SDBS) and sodium dodecylsulfate (SDS) were used. The powder dispersion of the resultant PPy was also observed to be dependent on the agitation speed and surfactant type. The morphology shown by SEM and TEM revealed that the anionic SDBS surfactant could effectively disperse into nanosized aggregates of the PPy. The results showed that the combination of the anionic surfactants and high agitation in the emulsion polymerization could produce nanosized PPy powders with higher conductivity.

Keywords Conductive polymer · Polypyrrole · Nanopowder · Homogenizer · Emulsion polymerization

Y. Hoshina · T. Kobayashi (✉)
Department of Materials Science and Technology, Nagaoka University of Technology,
1603-1 Kamitomioka, Nagaoka, Niigata 940-2188, Japan
e-mail: takaomi@nagaokaut.ac.jp

E. A. Zaragoza-Contreras
S.C. Laboratorio Nacional de Nanotecnologia, Centro de Investigación en Materiales Avanzados,
Miguel de Cervantes. No. 120, C.P. 31109 Chihuahua, Chih, Mexico

R. Farnood
Department of Chemical Engineering and Applied Chemistry, University of Toronto, 200 College
St., Toronto, ON M5S 3E5, Canada

Introduction

Polypyrrole (PPy) is an electrically conductive polymer that has attracted much attention recently because of its high conductivity, resistance to oxygen, thermal and environmental stability, and non-toxicity [1–5]. These characteristics are favorable for various applications, such as metallization of dielectrics, batteries, anticorrosive, electromagnetic shielding, sensors, and actuators [6–12]. However, several disadvantages exist and limit to use for a few applications. This is mainly because of their poor physical and mechanical properties as well as insolubility in common solvents as used for film preparation [13]. Therefore, modifications to conductive polymers might overcome these shortcomings. In order to overcome this problem, alkyl-chain-substituted pyrrole monomers have shown better solubility in common solvents. Furthermore, blending with other polymers and preparation of colloidal particles of conductive PPys have become typical methods for their modification. However, conductive polymer powders have also been applied to transparent conductive films dispersed in organic polymer sheets [14, 15]. To obtain such conductive polymer powders, emulsion polymerization has been reported as an effective method. Generally, it was known that the emulsion method used a bulky steric stabilizer to prevent aggregation of the conductive polymer [16–18]. The result indicated that this method was suitable for large-scale production of nanoparticles made of PPy and that it might constitute a simple and inexpensive approach. The preparation of nanosized powders, therefore, could present advantages for the improvement of the electrical and optical properties of the conductive polymers. Some research groups have prepared nanosized conductive polymers with a fine powder shape using microemulsion polymerization. For example, Reung-U-Rai et al. [19] reported that PPy particles of 60–90 nm were obtainable using this method. Stejskal and coworkers also studied the physical characteristics of PPy, reporting thermal stability and conductivity, when it was prepared in the presence of surfactants by using either anionic, cationic, or non-ionic types of surfactants [20, 21]. Furthermore, Xing et al. [22] demonstrated that an anionic surfactant such as sodium dodecylbenzene sulfonate used in the polymerization process of polymer products could strongly influence their morphology, thermal stability, and other properties. Although these works using surfactant for preparation of PPy powders have been investigated, little is known about researches of using surfactants with different changed species and non-ionic ones for pyrrole emulsion polymerization.

In addition, relative to above works of PPy powders, which have been already reported, agitation effect on preparation of PPy powders is still not studied. It is known that homogenizer is effective tool for mixing emulsion to prepare smaller sized polymers [23]. However, up to date, no reports about the impacts of homogenization on the emulsion polymerization for preparing nanosized PPy powders are performed. Therefore, we have paid attention of study for PPy nanoparticles affected by surfactant agitation in emulsion polymerization. In the present works, agitated emulsion polymerization with various surfactants under different stirring speeds was performed as original research for producing nanosized PPys. In detail, PPys were prepared by using homogenizer in the presence of anionic, cationic, or non-ionic surfactant, when emulsion polymerization was
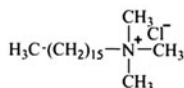
a. Anionic Surfactant

$H_3C\text{-}(CH_2)_{11}$ ⬡ $\text{-SO}_3^-Na^+$ **Sodium Dodecyl Benzene Sulfonate (SDBS)**
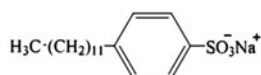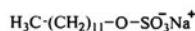
$H_3C\text{-}(CH_2)_{11}\text{-O-SO}_3^-Na^+$ **Sodium Dodecyl Sulfate (SDS)**

b. Cationic Surfactant

$H_3C\text{-}(CH_2)_{15}\text{-}\overset{CH_3}{\underset{CH_3}{\overset{+}{N}}}\text{-CH}_3 \; Cl^-$ **Cetyl Trimethyl Ammonium Chloride (CTAC)**

$R\text{-}\overset{CH_3}{\underset{CH_3}{\overset{+}{N}}}\overset{CH_2}{}Cl^-$ ⬡   **Benzalkonium Chloride (BAC)**

$R=C_8H_{17}\text{~}C_{18}H_{37}$
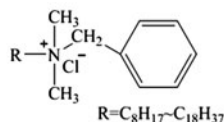
c. Non-ionic Surfactant
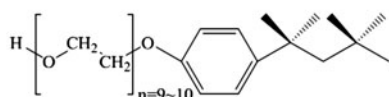
$H\left[O\text{-}\overset{CH_2}{\underset{CH_2}{}}\right]_{n=9\text{~}10}O\text{-}$ ⬡   **Polyethylene Glycol Mono-*p*-isooctylphenyl Ether (Triton X-100)**

Scheme 1 Chemical structures of surfactants

carried out at different agitation speeds of 650–24,000 rpm. Then, evidence of agitation effect on resultant nanosized PPys for their properties was investigated in the prospective dispersion and electrical conductivity.

Experimental

Materials

The pyrrole, used as monomer, was purchased from Tokyo Chemical Industry Co. Ltd. (Tokyo, Japan) and was distilled under reduced pressure after being dehydrated with calcium hydride for 24 h. Iron(III) chloride anhydrous ($FeCl_3$) was purchased from Nacalai Tesque Inc. (Tokyo, Japan) and used as an oxidant reagent. Five surfactants were used (Scheme 1). Sodium dodecylbenzene sulfonate (SDBS) and cetyl trimethyl ammonium chloride (CTAC) were from Tokyo Chemical Industry Co. Ltd. (Tokyo, Japan) and sodium dodecyl sulfate (SDS), benzalkonium chloride (BAC), and polyethylene glycol mono-*p*-isooctylphenyl ether (Triton X-100) were products of Nacalai Tesque Inc. (Tokyo, Japan). Distilled water was used for all experiments.

Preparation of PPy powders by emulsion polymerization
with and without different surfactants

Pyrrole (1.0 g, 14.9 mmol) was dissolved with its respective surfactant in 190 mL of distilled water inside a three-necked flask (500 mL). Here, the surfactant

Table 1 Polymerization yield, powder size distribution, and conductivity of PPy synthesized with or without each surfactant

Surfactant	Type	Concentration (mmol)	Mole fraction (–)	Yield (%)	Powder size distribution (µm)	Conductivity (S/cm)
	–	0	0	68	56–210	9.9×10^{-1}
SDBS	Anionic	0.2	0.01	74	23–160	5.9×10^{0}
		2	0.12	117	12–80	3.0×10^{1}
		5	0.25	139	5–54	3.1×10^{1}
		20	0.57	147	1–8	3.3×10^{1}
		40	0.73	150	1–12	3.3×10^{1}
SDS	Anionic	0.2	0.01	71	32–167	4.5×10^{0}
		2	0.12	113	14–83	1.2×10^{1}
		5	0.25	134	8–50	2.2×10^{1}
		20	0.57	142	3–19	2.4×10^{1}
		40	0.73	146	2–13	2.6×10^{1}
CTAC	Cationic	0.2	0.01	61	45–173	7.9×10^{-1}
		2	0.12	60	36–87	6.3×10^{-1}
		5	0.25	55	30–81	5.1×10^{-1}
		20	0.57	37	5–45	3.3×10^{-1}
		40	0.73	35	4–40	2.7×10^{-1}
BAC	Cationic	0.2	0.01	49	57–187	5.8×10^{-1}
		2	0.12	40	53–155	4.7×10^{-1}
		5	0.25	36	45–135	3.9×10^{-1}
		20	0.57	29	23–76	1.7×10^{-1}
		40	0.73	21	14–50	1.5×10^{-1}
TritonX-100	Non-ionic	0.2	0.01	62	57–192	9.1×10^{-1}
		2	0.12	53	55–174	8.3×10^{-1}
		5	0.25	48	51–167	7.3×10^{-1}
		20	0.57	41	45–159	4.1×10^{-1}
		40	0.73	35	36–113	8.5×10^{-2}

Stirring was carried out at 650 rpm. Pyrrole and oxidant as $FeCl_3$ amount were 1.0 g (14.9 mmol) and 5.6 g (34.5 mmol) in 200 mL reaction volume. Polymerization was for 2 h and these resultant polymer powders were weighted for calculation of yield

Mole fraction = mole of surfactant/(mole of surfactant + mole of pyrrole)

Yield (%) = (g of PPy/g of pyrrole) × 100, where g of PPy and g of pyrrole used weights of powder and monomer

concentration was varied between 0.2 and 40 mmol (Table 1). For dispersion at room temperature, either mechanical stirring at 650 rpm or agitation at 6,500, 13,500, or 24,000 rpm was performed using a homogenizer (L005470; IKA® Works, Inc., USA) for the pyrrole–water mixture. A similar procedure of pyrrole dispersion in water was conducted without surfactant as a reference. During the homogenization, $FeCl_3$ (5.6 g, 34.5 mmol) that had been dissolved in 10 mL of distilled water was added dropwise into the pyrrole/surfactant aqueous solution in

the reaction flask. The $FeCl_3$ added to the solution was functioned as the initiator of the pyrrole polymerization to obtain PPys [24, 25]. The polymerization was started immediately after the addition of $FeCl_3$ and proceeded as the solution changed color from transparent to black. Then the reaction was conducted for another 2 h at room temperature while maintaining agitation speeds. After the agitation was stopped, the precipitated black powders were centrifuged at 12,500 rpm and then washed with distilled water and acetone to remove remained monomer and other impurities. The obtained greenish black precipitates were dried in a vacuum oven at 60 °C for 12 h. The conditions used for preparations are listed in Table 1.

Measurements

For characterization of the resultant PPy powders, electrical conductivity, Fourier transform infrared (FT-IR) spectra, and UV–Visible absorption spectra were measured. For electrical conductivity, the dried PPy powders were compressed as pellets of 13 mm diameter and 1 mm thickness. Conductivity was measured using a typical four-point method (Roresta-GP MCP-T610; Mitsubishi Chemical Analytec Co. Ltd., Japan) at room temperature over the surface of the pellets. In all, five points on the surface of the pellets were selected to measure the conductivity. Then these values were averaged. FT-IR spectra of the resultant PPy powders were obtained using a FT-IR spectrometer (Prestige-21; Shimadzu Corp., Japan) in transmittance mode. Transmission spectra were obtained by forming a thin KBr-PPy pellet. The resolution of the spectral measurements was 4 cm^{-1} for each spectrum. The UV–Visible spectra of the PPy pellets were measured using a UV–VIS–NIR spectrophotometer (V-570; JASCO Corp., Japan) in reflection mode. Similarly, absorption spectra of the PPy powders dispersed in water were evaluated using absorption mode. To evaluate the powder size distribution, a laser diffraction particle size analyzer (SALD-7000; Shimadzu Corp., Japan) was also used on the aqueous dispersion solutions. The morphology of each polymer sample was observed using a scanning electron microscope (SEM, JSM-5300 LV; JEOL, Japan) after gold coating using a Quick cool coater (Sanyu Denshi K.K., Japan). Samples were also observed using a transmission electron microscope (TEM, JSM-7401F; JEOL, Japan).

Results and discussion

Polymerization of pyrrole in the presence of surfactant

To prepare PPy nanopowders in aqueous dispersion conditions, it has known that emulsion polymerization is an effective method for achievement of monomer dispersion with the aid of a surfactant in water [26, 27]. Therefore, in the present work, five surfactants, SDBS and others, were used for pyrrole polymerization in water. Table 1 presents some results obtained from the surfactants in the polymerization of pyrrole. For comparison of each PPy polymerization process, a different surfactant was used in the polymerization with stirring at 650 rpm.

Because the concentrations of the pyrrole monomer and $FeCl_3$ were fixed in the feed amounts, the surfactant concentration was also adjusted for each system. The polymerization was continued for 2 h in mechanical stirring conditions. The values for the yield of the PPy, when anionic surfactants such as SDBS and SDS were used, tended to increase with the increased surfactant amounts. Especially, although the resultant PPy was well washed with excess water and acetone after polymerization, the resultant values of yield were still greater than 100%, except when the concentration was higher than 0.2 mmol. This indicated that the presence of un-removed surfactant might result from the formation of an anion–cation complex with the surfactant and the resultant PPy powders. However, the use of cationic and non-ionic surfactants tended to decrease the yields of PPy when the surfactant concentration was high. Consequently, the anionic and cationic surfactants affected the yields of the PPy in the emulsion polymerization. Table 1 shows values of conductivity (S/cm) for the PPy pellets and the powder size distribution observed in water. Actually, the anionic surfactant systems showed a tendency to have higher conductivity relative to those of the reference. Regarding the increase in the concentrations in the SDBS and SDS systems, the observed conductivity was in the range of about 5.9–33 and 4.5–26 S/cm, respectively, from 0.2 to 40 mmol. This phenomenon reflected that extending conjugate chains of the PPy was present and that a high degree of acceptor doping of a form of the DBS^- or DS^- ion was introduced electrostatically into the polymer powders. Additionally, for the reference PPy, the Cl^- ion was introduced by $FeCl_3$ oxidant in the polymerization and was able to act as a dopant when the cationic or non-ionic surfactant was used. However, the resultant conductivities of CTAC, BAC, and Triton X-100 were lower than those of the anionic surfactants. Consequently, the PPy conductivity differed according to the species of surfactant used as the chemical dopant.

Because the conductivity depended strongly upon the species of surfactants that were used, the FT-IR spectra of the PPy synthesized with and without surfactant were measured to detect the presence of the surfactant. Figure 1A shows FT-IR spectra of PPys obtained with and without surfactant. These data showed the appearance of the characteristic PPy bands for the C=C double bond stretching of the aromatic ring (1,545 cm^{-1}), the C–N stretching vibration (1,454 cm^{-1}), and both peaks of the =CH– in-plane vibration (1,300 cm^{-1}) and vibration of the pyrrole ring (1,190 cm^{-1}). The bands at about 1,030 and 904 cm^{-1} were attributed to the C–H and N–H in-plane deformation vibrations. Furthermore, C–H stretching between 2,850 and 2,950 cm^{-1} was observed for the PPy-anionic surfactant systems such as PPy–SDBS and PPy–SDS. This resulted from effects of the doping the anionic surfactant in the PPy. As Fig. 1B showed, the IR band intensity of the C–H stretching for the long alkyl group of the dodecyl benzene increased with increased the surfactant feeding in the polymerization process. We estimated contents of the SDBS in the PPy using the composition of the IR bands of SDBS and PPy. The IR intensity of the characteristic bands of 2,925 and 1,545 cm^{-1} for SDBS and PPy were compared. Results showed that the mole fractions of DBS^- in the PPy were 2.0, 2.9, 4.4, 5.7, and 5.8 mol%, as inferred from the SDBS concentration variation in the polymerization at 0.2, 2, 5, 20, and 40 mol. Figure 2A portrays UV–Vis spectra of the PPy pellets prepared with and without surfactant. The resultant
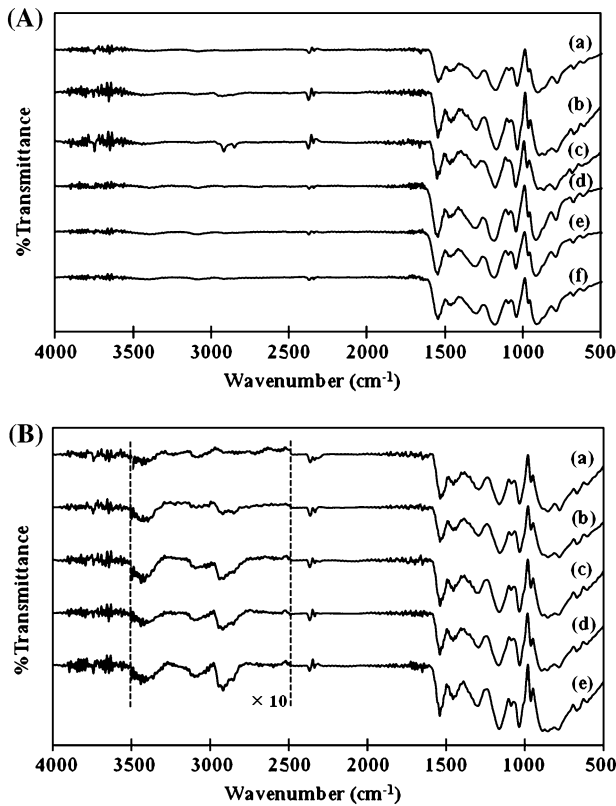
Fig. 1 A FT-IR spectra of the PPy (*a*) without surfactant and with (*b*) SDBS, (*c*) SDS, (*d*) CTAC, (*e*) BAC, and (*f*) Triton X-100. The surfactant feed was 20 mmol in the emulsion polymerization at 650 rpm. **B** FT-IR spectra of the PPy with SDBS of (*a*) 0.2 mmol, (*b*) 2 mmol, (*c*) 5 mmol, (*d*) 20 mmol, and (*e*) 40 mmol

UV–Vis spectra of the SDBS–PPy and SDS–PPy systems measured in reflection mode showed that a characteristic weaker absorption band appeared near 370–430 nm. A stronger and broadening absorption was observed for 600–850 nm. The absorption band at 370–430 nm was associated with the π–π^* transition of the PPy. The strong and broad bands in 600–850 nm were assigned to the bipolaron state of PPy [28]. Figure 2B also shows the reflection UV–Vis spectra of the PPy obtained using different SDBS feeds. Data showing broadening absorption of the bipolaron state were observed clearly in 600–850 nm region, when the surfactant concentration became higher for the SDBS–PPy system. The maximum wavelength of the bipolaron state was shifted from 630 to 700 nm when the SDBS was fed from 0.2 to 40 mmol, respectively, in the polymerization. These observations revealed that the anionic surfactant used for the polymerization acted as the dispersion reagent incorporated itself into the PPy backbones as a doping agent became of the formation of the SO_3^-–Py complex.
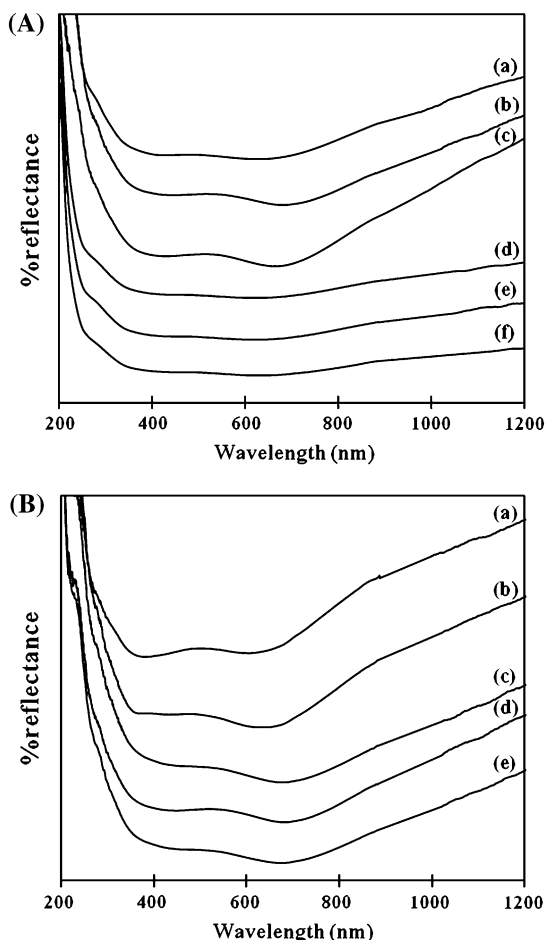
Table 1 shows the powder size distribution of the PPy dispersed in water. In addition, Fig. 3 shows the relative size distribution of the resultant PPy powders for SDBS, CTAC, and Triton X-100 systems at different concentrations in water. As shown there, the powder size distribution of the PPys was shifted to the smaller side when the SDBS concentration increased. Especially, the PPy dispersion of the SDBS–PPy was effective with less than 2 mmol contents. As shown, the average powder size for the SDBS–PPy and SDS–PPy systems was decreased considerably by increasing the surfactant concentration. This was mainly because of the dopant of anionic species stabilizing the resultant PPy particles through the formation of the ionic complex. However, other systems used with cationic and non-ionic were observed similarly, but the powder size distribution became broader and larger relative to that of the SDBS–PPy system, perhaps because of the low ability to achieve dispersion stability of the PPy without such an ion complex for the cases of CTAC and Triton X-100.
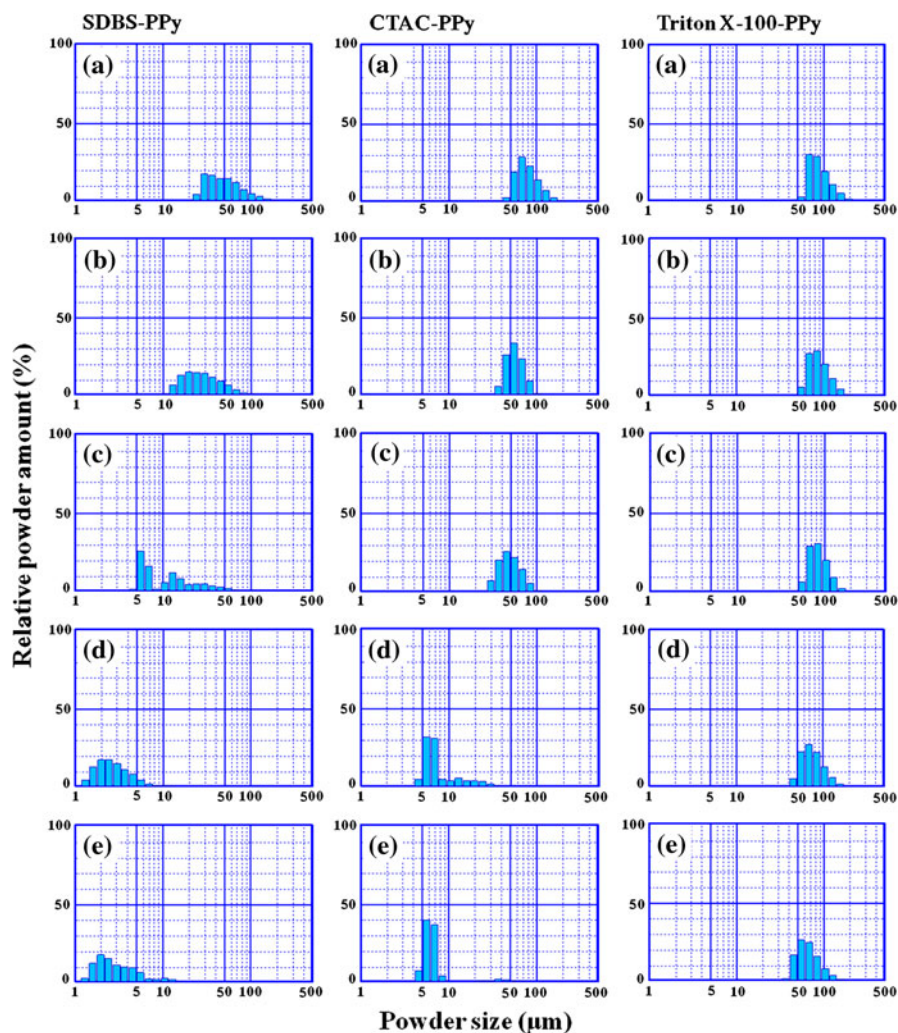
Fig. 3 Powder size distribution of the PPy with SDBS, CTAC and Triton X-100 of **a** 0.2 mmol, **b** 2 mmol, **c** 5 mmol, **d** 20 mmol, and **e** 40 mmol at 650 rpm

Effects of agitation on the resultant PPy powders

To elucidate agitation speed effects on the emulsion polymerization of the PPy, polymerization was conducted at speeds greater than 650 rpm using a homogenizer. As portrayed in Fig. 4, the yields obtained for the non-surfactant system at 6,500–24,000 rpm were 68–64%. High agitation lowered the yield of the PPy slightly relative to data obtained with 650 rpm stirring. When SDBS was added to the polymerization, higher yields of 149–147% were obtained. These values were higher than those of either cationic or non-ionic systems. For the yield of the SDS–PPy system, somewhat lower values were observed. Figure 5 shows the effect of the
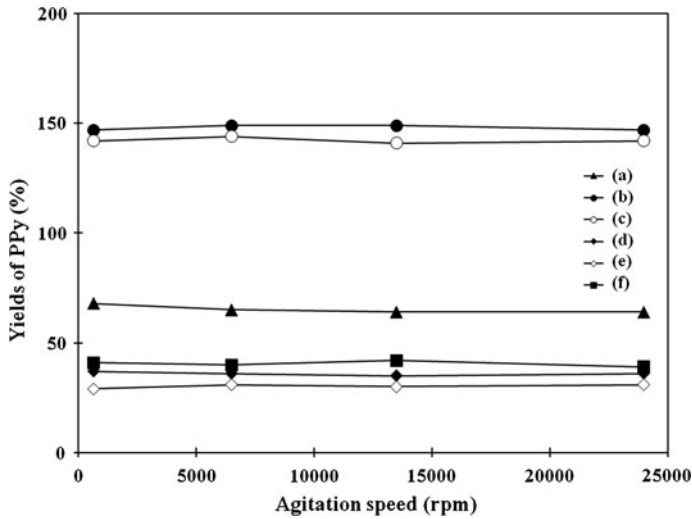
Fig. 4 Agitation speed of polymerization and yield of the PPy prepared (*a*) without surfactant and with (*b*) SDBS, (*c*) SDS, (*d*) CTAC, (*e*) BAC, and (*f*) Triton X-100 by 20 mmol feed
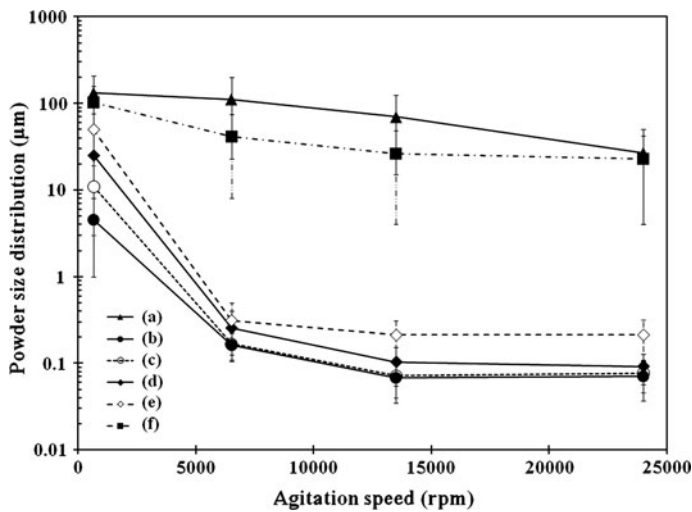

Fig. 5 Agitation speed of polymerization and powder size distribution of the PPy prepared (*a*) without surfactant and with (*b*) SDBS, (*c*) SDS, (*d*) CTAC, (*e*) BAC, and (*f*) Triton X-100 by 20 mmol feed

agitation speed on the yield and other properties of the PPy nanopowders. In the polymerization experiments, the agitation speed of the homogenizer was changed from 6,500 to 24,000 rpm, with fixed concentrations of the surfactant and pyrrole. In the SDBS–PPy system, the powder size distribution was shifted to a smaller size of about 35–102 and 37–104 nm, because the respective speeds were 13,500 and 24,000 rpm. The SDS–PPy system showed a similar tendency, with 40–103 and
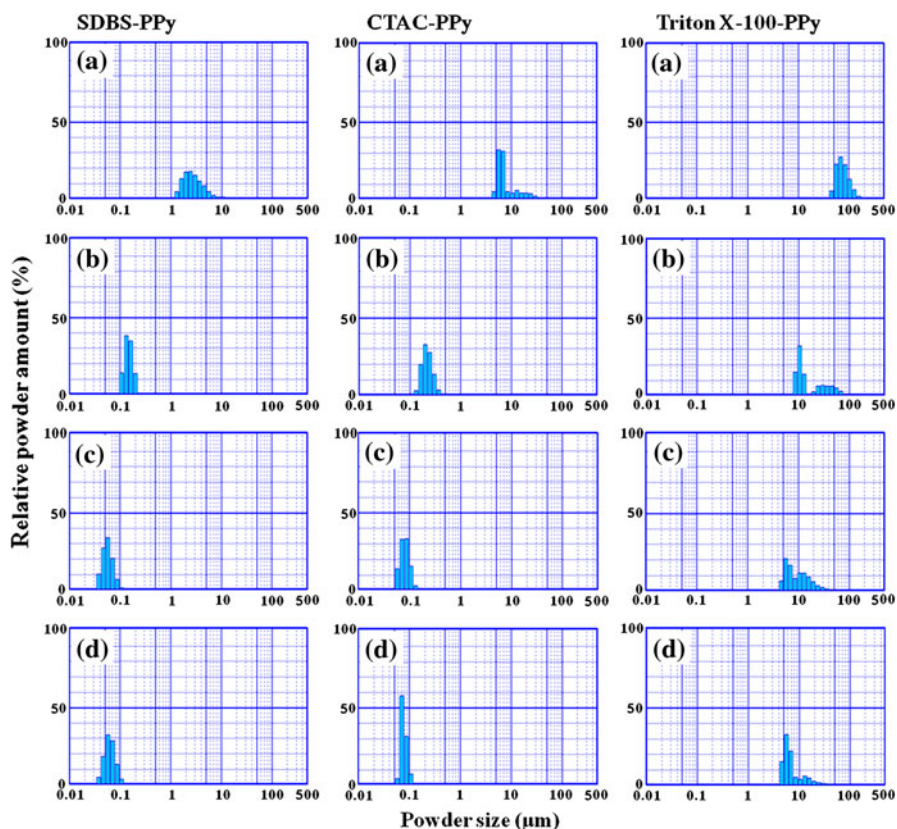
Fig. 6 Powder size distribution of the PPy prepared with SDBS, CTAC, and Triton X-100 (20 mmol feed) at **a** 650 rpm, **b** 6,500 rpm, **c** 13,500 rpm, and **d** 24,000 rpm

46–107 nm observed, respectively, for 13,500 and 24,000 rpm. In contrast, the CTAC–PPy system showed about 55–152 and 57–127 nm for respective agitation speeds of 13,500 and 24,000 rpm, but the effect was apparently lower than in the cases of the SDBS–PPy and SDS–PPy systems. The non-ionic surfactant for the Triton X-100–PPy system showed a somewhat larger powder diameter than that obtained using the SDBS–PPy system. The powder particle size distributions were about 8–75, 4–48, and 4–42 μm, respectively, for specimens agitated at 6,500, 13,500, and 24,000 rpm when a Triton X-100 was used. As Fig. 6 shows, the powder size distribution of the PPy powders shifted significantly to the lower side, as obtained using the higher agitation for the SDBS–PPy and the CTAC–PPy systems. Although it was not observed well for the case of Triton X-100–PPy systems, these data showed clearly that the agitation speed was effective for the production of PPy nanosize powders.

Figure 7 presents results for the electrical conductivity of PPy powders obtained at different agitation speeds. The conductivity of the resultant PPy pellets did not vary significantly in the absence and presence of surfactant at different agitation speeds. In the absence of the surfactant, the pellet showed conductivity of
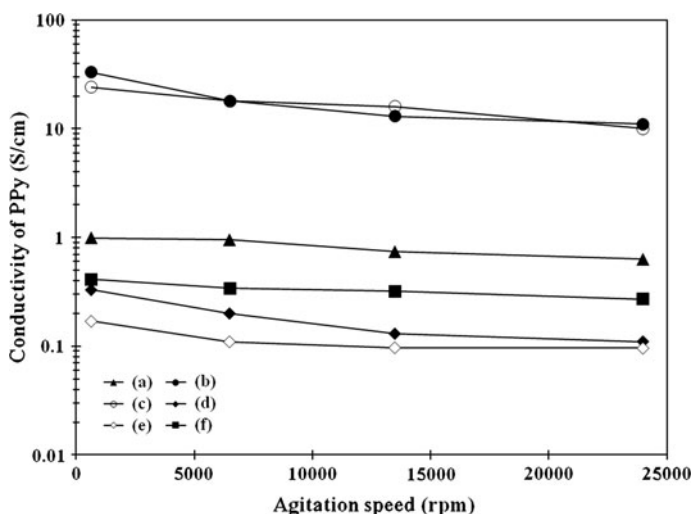
Fig. 7 Agitation speed of polymerization and conductivity of the PPy prepared (*a*) without surfactant and with (*b*) SDBS, (*c*) SDS, (*d*) CTAC, (*e*) BAC, and (*f*) Triton X-100 by 20 mmol feed

9.9×10^{-1} S/cm, which might result from the Cl^- ion being a less effective dopant added from the $FeCl_3$ oxidant. In contrast, it was a remarkable observation for the cases of the anionic surfactants of SDBS–PPy and the SDS–PPy systems that the conductivities obtained appeared at 4–33 S/cm. This more clearly showed that the effect of the dopant using an anionic surfactant caused higher conductivity.

Examination of the dispersion conditions of resultant PPy powders prepared with different agitation speeds in the absence and presence of the surfactants is important. The morphology of the PPy powders was observed by SEM and TEM measurements. Figures 8 and 9 portray SEM and TEM images of the resultant PPy powders. Here, these PPys were prepared with agitation speeds of 650 and 13,500 rpm using the homogenizer. When no surfactant was present in the polymerization medium (Fig. 8a), the resultant PPy showed strong aggregation, with about 300 nm size of the aggregates. The SEM image (b) of the SDBS–PPy powders appeared to show more compact particles, of about 60 nm, relative to those of the other images (a). However, the images of PPy powders of the CTAC–PPy and Triton X-100 systems showed powder sizes around 100–200 nm. In panels (e)–(h) for the PPy powders obtained at 13,500 rpm, it was clarified that the dispersion effectively enhanced for the obtained size of the PPy particles. As shown in Fig. 9, which depicts TEM images, the smaller PPy powder particles were mutually aggregated. For panels (a) and (b) of the PPy prepared without surfactant, some particles that were present in an aggregated condition had about 40–55 nm diameter. However, the aggregated size of the SDBS–PPy system obtained with 13,500 rpm formed small aggregates of the nanosized PPy powders about 35–50 nm. These results demonstrated that, at high agitation speed, the SDBS surfactant could disperse the PPy well. At these conditions, the agitation speed enhanced the production of nanosized PPy with good dispersion. Relative to the cationic and non-ionic surfactants, the anionic surfactants at high-speed agitation
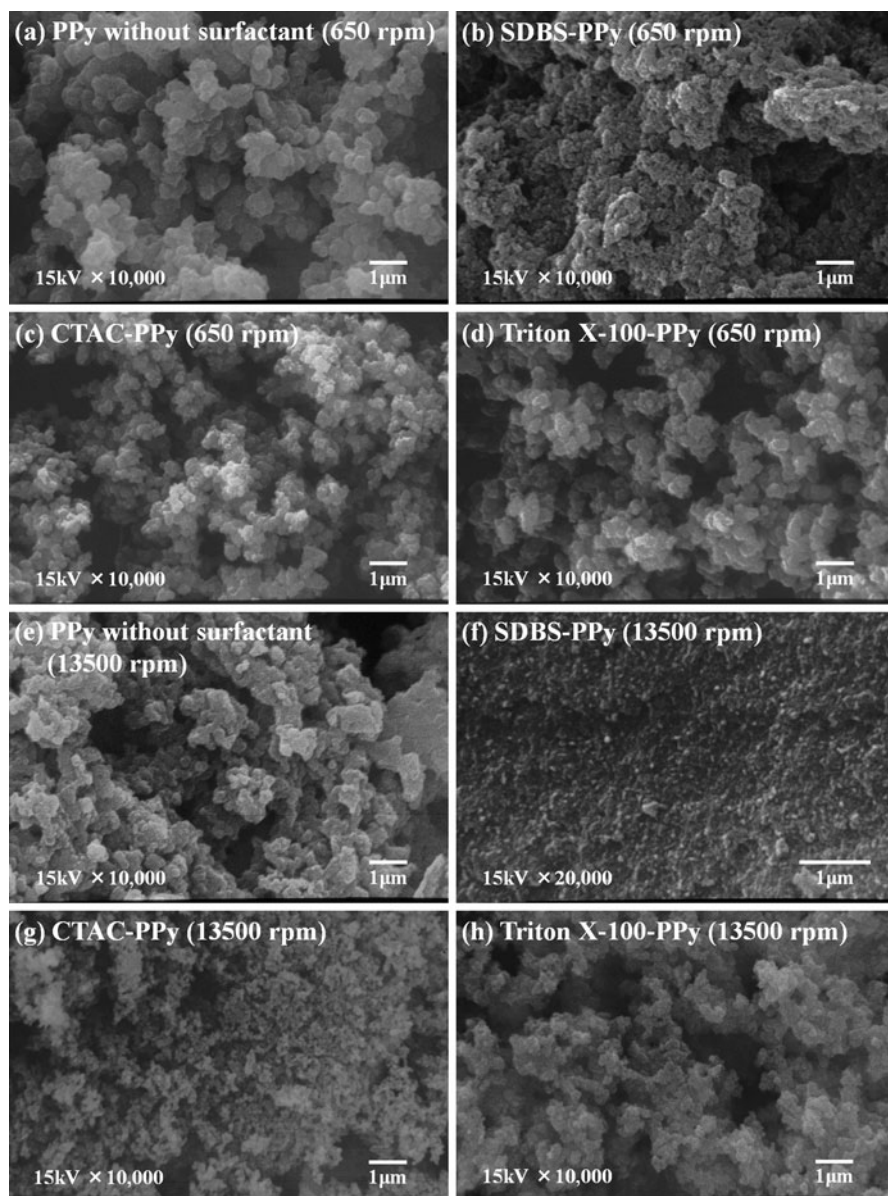
Fig. 8 SEM images of the PPy without surfactant and with SDBS, CTAC, and Triton X-100. Each surfactant was 20 mmol for emulsion polymerization at 650 (**a–d**) and 13,500 rpm (**e–h**)

were extremely effective for the dispersion, meaning that the dopant surfactant produced a bipolaron state, which then resulted in the high conductivity. As evidence of these results, although the obtained polymer powders could not be dissolved in organic solvents, the resultant nanosized powders were well dispersed in water.
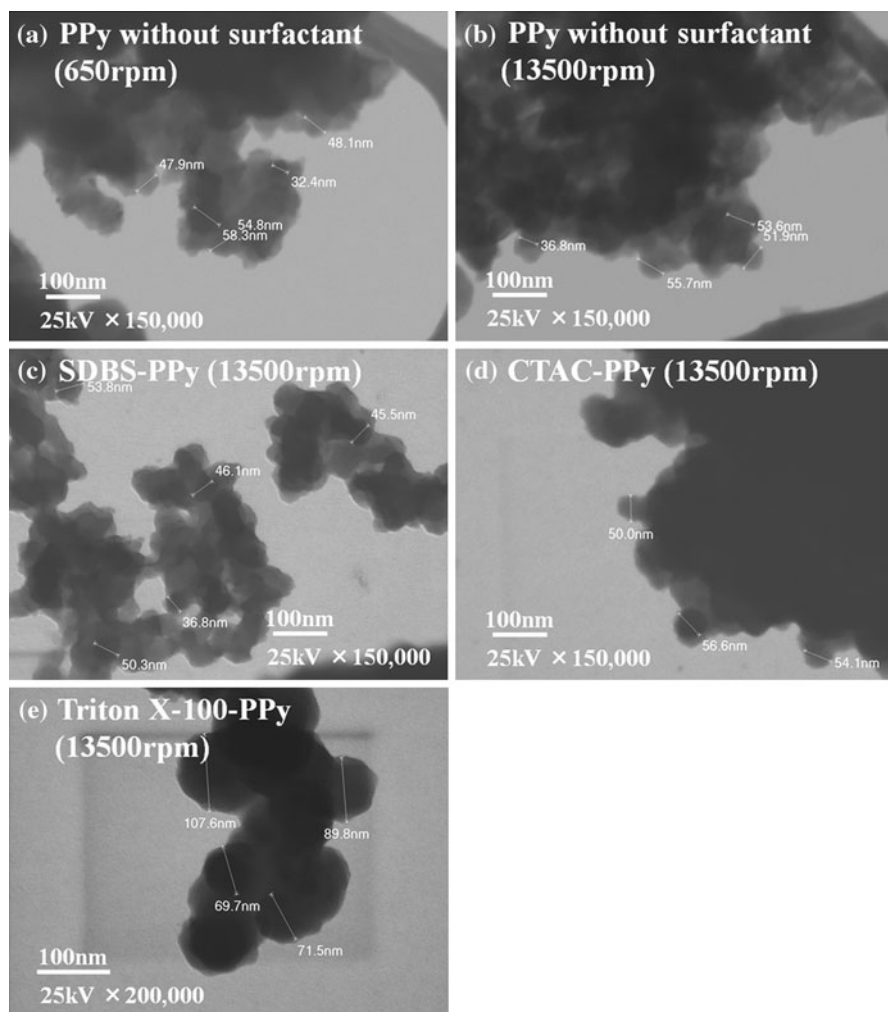
Fig. 9 TEM images of the PPy without surfactant synthesized at **a** 6,500 and **b** 13,500 rpm and with **c** SDBS, **d** CTAC, and **e** Triton X-100. Each surfactant was 20 mmol for the emulsion polymerization at 13,500 rpm

It might be possible to measure the absorption spectra using transmittance mode. For example, in the spectra for the SDBS–PPy solution in Fig. 10A, absorption bands were observed at 460 nm in the UV–Vis spectrum and at around 900 nm for stronger broad absorption. The first absorption band was associated with the $\pi-\pi^*$ transition band, whereas the second was associated with the bipolaron state of PPy [18, 29]. However, for the non-surfactant system and CTAC–PPy and Triton X-100 systems, we were unable to prepare such transparent solutions with the produced PPys in the aqueous solution. As shown in Fig. 10B, the UV–Vis spectra of SDBS–PPy solution became shaped clearly with the effect of dispersion of PPy at high agitation speed.

Fig. 10 A UV–Visible spectra of the PPy aqueous solution for the polymer (*a*) without surfactant and with (*b*) SDBS, (*c*) CTAC, and (*d*) Triton X-100. The PPy was prepared with 20 mmol surfactant feed at 13,500 rpm. **B** UV–Visible spectra of the PPy aqueous solution for the polymer with SDBS at (*a*) 650 rpm, (*b*) 6,500 rpm, (*c*) 13,500 rpm and (*d*) 24,000 rpm
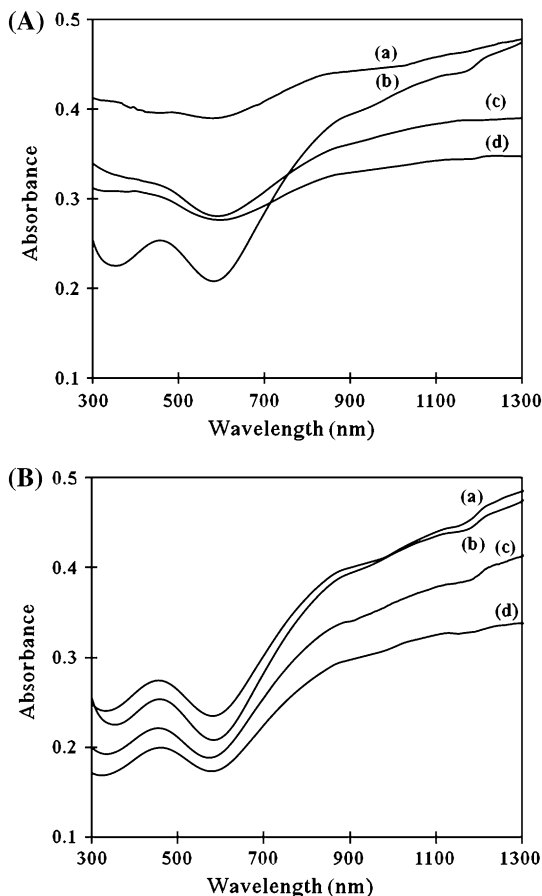
Conclusion

In the present work, nanosized PPy powders were prepared at high agitation speeds using emulsion polymerization of pyrrole with anionic surfactants used as dopants. The PPy produced with anionic surfactant SDBS had about 30 S/cm conductivity with aggregation powders having particle sizes of about 1–8 μm. The results of FT-IR and UV–Visible spectra proved that the surfactant was incorporated into the PPy backbone with ionic complex formation as the doping anion. Additionally, the increment of the dopant engendered high conductivity, as observed in the resultant PPy. In contrast, the PPy prepared without surfactant and with cationic and non-ionic-PPy systems showed less conductivity, resulting in less dopant ability for their surfactants. For agitation speeds of 13,500–24,000 rpm using homogenizer for the SDBS–PPy system, the PPy powders were well dispersed: 35–102 nm. However, CTAC and Triton X-100 showed very low dispersion and lower conductivity in the resultant PPy powders.

References

1. Tourillion G, Garnier F (1982) New electrochemically generated organic conducting polymers. J Electroanal Chem 135:173–178
2. Joo J, Lee JK, Lee SY, Jang KS, Oh EJ, Epstein AJ (2000) Physical characterization of electrochemically and chemically synthesized polypyrroles. Macromolecules 33:5131–5136
3. Romero AJF, Cascales JJL, Otero TF (2005) Perchlorate interchange during the redox process of PPy/PVS films in an acetonitrile medium. A voltammetric and EDX study. J Phys Chem B 109:907–914
4. Carrasco PM, Grande HJ, Cortazar M, Alberdi JM, Areizaga J, Pomposa JA (2006) Structure-conductivity relationships in chemical polypyrroles of low, medium and high conductivity. Synth Met 156:420–425
5. Yang C, Liu P (2009) Water-dispersed conductive polypyrroles doped with lignosulfonate and the weak temperature dependence of electrical conductivity. Ind Eng Chem Res 48:9498–9503
6. Intelmann CM, Syritski V, Tsankov D, Hinrichs K, Rappich J (2008) Ultrathin polypyrrole films on silicon substrates. Electrochim Acta 53:4046–4050
7. Niside H, Oyaizu K (2008) Toward flexible batteries. Science 319:737–738
8. Lenz DM, Delamar M, Ferreira C (2003) Application of polypyrrole/TiO_2 composite films as corrosion protection of mild steel. J Electroanal Chem 540:35–44
9. Nguyen MT, Diaz AF (1994) A novel method for the preparation of magnetic nanoparticles in a polypyrrole powder. Adv Mater 6:858–860
10. Ghanbari K, Bathaie SZ, Mousavi MF (2008) Electrochemically fabricated polypyrrole nanofiber-modified electrode as a new electrochemical DNA biosensor. Biosens Bioelectron 23:1825–1831
11. Lopez-Crapez E, Livache T, Marchand J, Grenier J (2001) K-ras mutation detection by hybridization to a polypyrrole DNA chip. Clin Chem 47:186–194
12. Jager EWH, Smela E, Inganäs O (2000) Microfabricating conjugated polymer actuators. Science 290:1540–1545
13. Wang LX, Li XG, Yang YL (2001) Preparation, properties and applications of polypyrroles. React Funct Polym 47:125–139
14. Gospodinova N, Mokreva P, Tsanov T, Terlemezyan L (1997) A new route to polyaniline composites. Polymer 38:743–746
15. Jang J, Oh JH, Stucky GD (2002) Fabrication of ultrafine conducting polymer and graphite nanoparticles. Angew Chem Int Ed 41:4016–4019
16. DeArmitt C, Armes SP (1993) Colloidal dispersions of surfactant-stabilized polypyrrole particles. Langmuir 9:652–654
17. Luk SY, Lineton W, Keane M, DeArmitt C, Armes SP (1995) Surface composition of surfactant-stabilised polypyrrole colloids. J Chem Soc Faraday Trans 91:905–910
18. Stejskal J (2001) Colloidal dispersions of conducting polymers. J Polym Mater 18:225–258
19. Reung-U-Rai A, Prom-Jun A, Prissanaroon-Ouajai W, Ouajai S (2008) Synthesis of highly conductive polypyrrole nanoparticles via microemulsion polymerization. J Met Mater Miner 18:27–31
20. Stejskal J, Omastová M, Fedorova S, Prokes J, Trchova M (2003) Polyaniline and polypyrrole prepared in the presence of surfactants: a comparative conductivity study. Polymer 44:1353–1358
21. Omastová M, Trchová M, Kovářová J, Stejskal J (2003) Synthesis and structural study of polypyrroles prepared in the presence of surfactants. Synth Met 138:447–455
22. Xing S, Zhao G (2006) Morphology and thermostability of polypyrrole prepared from SDBS aqueous solution. Polym Bull 57:933–943
23. Zhao H, Gagnon J, Häfeli UO (2007) Process and formulation variables in the preparation of injectable and biodegradable magnetic microspheres. Biomagn Res Technol 5:2
24. Myers RE (1986) Chemical oxidative polymerization as a synthetic route to electrically conducting polypyrroles. J Electron Mater 15:61–69
25. Thieblemont JC, Brun A, Marty J, Planche MF, Calo P (1995) Thermal-analysis of polypyrrole oxidation in air. Polymer 36:1605–1610
26. Berdichevsky Y, Lo YH (2006) Polypyrrole nanowire actuators. Adv Mater 18:122–125
27. Huang J, Virji S, Weiller BH, Kaner RB (2004) Nanostructured polyaniline sensors. Chem Eur J 10:1314–1319

28. Crowley K, Cassidy J (2003) In situ resonance Raman spectroelectrochemistry of polypyrrole doped with dodecylbenzenesulfonate. J Electroanal Chem 547:75–82
29. Jang KS, Lee H, Moon B (2004) Synthesis and characterization of water soluble polypyrrole doped with functional dopants. Synth Met 143:289–294